Stereospecific Alkane Hydroxylation by Non-Heme Iron Catalysts: Mechanistic Evidence for an Fe^{V}═O Active Species

Kui Chen and Lawrence Que, Jr.*

Contribution from the Department of Chemistry and Center for Metals in Biocatalysis, University of Minnesota, 207 Pleasant Street SE, Minneapolis, Minnesota 55455

Received February 5, 2001

Abstract: High-valent iron−oxo species have frequently been invoked in the oxidation of hydrocarbons by both heme and non-heme enzymes. Although a formally Fe^{V}═O species, that is, $[(Por^{\bullet})Fe^{IV}{=}O]^{+}$, has been widely accepted as the key oxidant in stereospecific alkane hydroxylation by heme systems, it is not established that such a high-valent state can be accessed by a non-heme ligand environment. Herein we report a systematic study on alkane oxidations with H_2O_2 catalyzed by a group of non-heme iron complexes, that is, $[Fe^{II}(TPA)(CH_3CN)_2]^{2+}$ (**1**, TPA = tris(2-pyridylmethyl)amine) and its α- and β-substituted analogues. The reactivity patterns of this family of Fe^{II}(TPA) catalysts can be modulated by the electronic and steric properties of the ligand environment, which affects the spin states of a common Fe^{III}−OOH intermediate. Such an Fe^{III}−peroxo species is high-spin when the TPA ligand has two or three α-substituents and is proposed to be directly responsible for the selective C−H bond cleavage of the alkane substrate. The thus-generated alkyl radicals, however, have relatively long lifetimes and are susceptible to radical epimerization and trapping by O_2. On the other hand, **1** and the β-substituted Fe^{II}(TPA) complexes catalyze stereospecific alkane hydroxylation by a mechanism involving both a low-spin Fe^{III}−OOH intermediate and an Fe^{V}═O species derived from O−O bond heterolysis. We propose that the heterolysis pathway is promoted by two factors: (a) the low-spin iron(III) center which weakens the O−O bond and (b) the binding of an adjacent water ligand that can hydrogen bond to the terminal oxygen of the hydroperoxo group and facilitate the departure of the hydroxide. Evidence for the Fe^{V}═O species comes from isotope-labeling studies showing incorporation of ^{18}O from $H_2{}^{18}O$ into the alcohol products. ^{18}O-incorporation occurs by $H_2{}^{18}O$ binding to the low-spin Fe^{III}−OOH intermediate, its conversion to a *cis*-$H^{18}O$−Fe^{V}═O species, and then oxo−hydroxo tautomerization. The relative contributions of the two pathways of this dual-oxidant mechanism are affected by both the electron donating ability of the TPA ligand and the strength of the C−H bond to be broken. These studies thus serve as a synthetic precedent for an Fe^{V}═O species in the oxygen activation mechanisms postulated for non-heme iron enzymes such as methane monooxygenase and Rieske dioxygenases.

High-valent iron−oxo species have been proposed as key intermediates in biological hydrocarbon oxidations. Prime examples are those found for the porphyrin-containing cytochrome P450,[1,2] the non-heme diiron enzyme methane monooxygenase,[3] and the non-heme mononuclear iron-containing Rieske dioxygenases.[4] For cytochrome P450, the two oxidizing equivalents required for stereoselective hydrocarbon oxidations are stored on the metal center and the porphyrin, and the active species is formulated as $[(Por^{\bullet})Fe^{IV}{=}O]^{+}$.[1,2] The corresponding intermediate in methane monooxygenase has an $Fe^{IV}{}_2(\mu\text{-}O)_2$ core where the second iron assumes the role of the porphyrin radical,[5,6] but some theoretical calculations speculate that the $Fe^{IV}{}_2(\mu\text{-}O)_2$ core isomerizes to a more reactive Fe^{III}−O−Fe^{V}═O form prior to attack of the methane C−H bond.[7,8] A mononuclear Fe^{V}═O species has also been proposed for Rieske dioxygenases to carry out stereospecific alkane hydroxylation and alkene *cis*-dihydroxylation reactions, although no active species has been characterized in the enzymatic cycle.[4,9] In model studies of non-heme iron enzymes, high-valent iron−oxo species have frequently been invoked in biomimetic hydrocarbon oxidations by iron catalysts.[10−12] However, no experimental evidence has been obtained for an active Fe^{V}═O species in a non-heme ligand environment, in contrast to the well characterized $[(Por^{\bullet})Fe^{IV}{=}O]^{+}$ intermediate in heme sys-

* To whom correspondence should be addressed. E-mail: que@chem.umn.edu. Fax: 612-624-7029.

(1) Groves, J. T.; Han, Y.-Z. In *Cytochrome P-450. Structure, Mechanism, and Biochemistry*, 2nd ed.; Ortiz de Montellano, P. R., Ed.; Plenum Press: New York, 1995; pp 3−48.

(2) Schlichting, I.; Berendzen, J.; Chu, K.; Stock, A. M.; Maves, S. A.; Benson, D. E.; Sweet, R. M.; Ringe, D.; Petsko, G. A.; Sligar, S. G. *Science* **2000**, *287*, 1615−1622.

(3) Wallar, B. J.; Lipscomb, J. D. *Chem. Rev.* **1996**, *96*, 2625−2658.

(4) Que, L., Jr.; Ho, R. Y. N. *Chem. Rev.* **1996**, *96*, 2607−2624.

(5) Shu, L.; Nesheim, J.; Kauffmann, K.; Münck, E.; Lipscomb, J. D.; Que, L., Jr. *Science* **1997**, *275*, 515−518.

(6) Lipscomb, J. D.; Que, L., Jr. *J. Biol. Inorg. Chem.* **1998**, *3*, 331−336.

(7) Siegbahn, P. E. M.; Crabtree, R. H. *J. Am. Chem. Soc.* **1997**, *119*, 3103−3113.

(8) Siegbahn, P. E. M.; Crabtree, R. H.; Nordlund, P. *J. Biol. Inorg. Chem.* **1998**, *3*, 314−317.

(9) Wolfe, M. D.; Parales, J. V.; Gibson, D. T.; Lipscomb, J. D. *J. Biol. Chem.* **2001**, *276*, 1945−1953.

(10) Fontecave, M.; Ménage, S.; Duboc-Toia, C. *Coord. Chem. Rev.* **1998**, *178−180*, 1555−1572.

(11) Shilov, A. E.; Shteinman, A. A. *Acc. Chem. Res.* **1999**, *32*, 763−771.

(12) Costas, M.; Chen, K.; Que, L., Jr. *Coord. Chem. Rev.* **2000**, *200−202*, 517−544.

10.1021/ja010310x CCC: $20.00
Published on Web 06/09/2001

Scheme 1. Non-Heme Ligands Studied in This Paper and the Numbering of the Corresponding Mononuclear Iron(II) Complexes

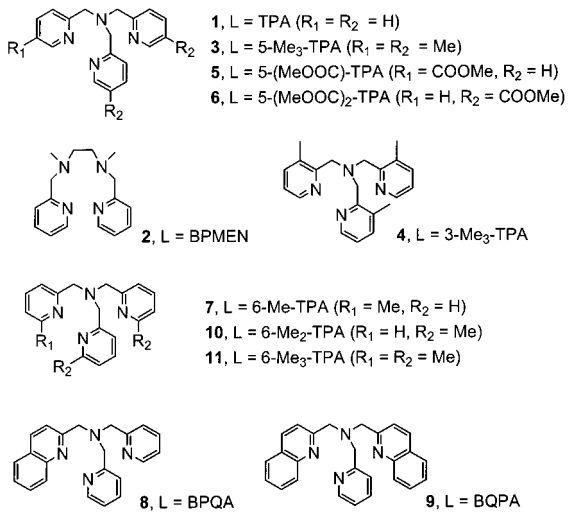

tems.[1,13] These results raise the question of whether a formally iron(V) oxidation state can be attained in the absence of a porphyrin ligand.

In the course of developing functional models for non-heme iron oxygenases, we have discovered a family of non-heme iron catalysts, represented by $[Fe^{II}(TPA)(CH_3CN)_2]^{2+}$ (**1**, TPA = tris-(2-pyridylmethyl)amine, Scheme 1), that are capable of stereospecific hydrocarbon oxidations with H_2O_2 as the oxidant.[14,15] Here we present a detailed study of alkane hydroxylation by these catalysts that provides strong mechanistic evidence for the involvement of a formally iron(V)−oxo species in a non-heme iron system.

Experimental Section

Materials. All reagents were purchased from Aldrich and used as received unless noted otherwise. $H_2{}^{18}O$ (85% or 96.5% ^{18}O-enriched), $H_2{}^{18}O_2$ (90% ^{18}O-enriched, 2% solution in $H_2{}^{16}O$), and $^{18}O_2$ (96% ^{18}O-enriched) were obtained from ICON, NJ. $H_2{}^{18}O$ (88.8% or 98.6% ^{18}O-enriched) was obtained from Isotec. *trans*-1,2-Dimethylcyclohexane was purified by distillation. Cyclohexane, cyclooctane, and *cis*-1,2-dimethylcyclohexane were passed through silica gel before the reactions. The epimeric tertiary alcohols of 1,2-dimethylcyclohexanes or decalins were obtained by the stereospecific hydroxylation of the corresponding alkane substrate by Fe^{III}(TPP)Cl (TPP = 5,10,15,20-tetraphenylporphinato dianion) and PhIO.[16]

Syntheses. The ligands 5-Me_3-TPA,[17] 3-Me_3-TPA,[18] 5-(MeOOC)-TPA,[19] BPQA,[20] and BQPA[20] were obtained according to literature procedures. Iron complexes $[Fe^{II}(TPA)(CH_3CN)_2](ClO_4)_2$ (**1**),[21] $[Fe^{II}(BPMEN)(CH_3CN)_2](ClO_4)_2$ (**2**),[15] $[Fe^{II}(6\text{-}Me_n\text{-}TPA)(CH_3CN)_2](ClO_4)_2$ (**7**, $n = 1$; **10**, $n = 2$; **11**, $n = 3$),[21] $[Fe^{III}_2(\mu\text{-}O)(TPA)_2(H_2O)_2](ClO_4)_4$ (**1a**),[17] $[Fe^{II}(N4Py)(CH_3CN)](ClO_4)_2$ (**12**),[22] $[Fe^{III}(TPA)Cl_2](ClO_4)$ (**1b**),[23a] $[Fe^{III}(TPA)Br_2](ClO_4)$,[23a] $[Fe_2^{III}O(TPA)_2(O_2CCH_3)](ClO_4)_3$,[23b] and $[Fe_2^{III}O(TPA)_2(O_2CPh)](ClO_4)_3$[23b] were synthesized as reported.

Bis[(5-methoxycarbonyl-2-pyridyl)methyl](2-pyridylmethyl)-amine (5-(MeOOC)$_2$-TPA). Methyl 6-bromomethylnicotinate (1.05 g, 4.57 mmol)[19] was dissolved in 100 mL of anhydrous DMF under N_2 atmosphere. Into this solution was added 0.25 g of (2-pyridylmethyl)-amine (2.29 mmol) and 0.82 g of Cs_2CO_3 (2.52 mmol). The mixture was stirred at room temperature under N_2 atmosphere overnight, followed by filtration of the CsBr solid residue and vacuum distillation of solvent. The resulting oil was further purified by column chromatography using Al_2O_3 and eluting with 1% $CH_3OH/CHCl_3$ ($R_f = 0.8$, alumina, 5% $CH_3OH/CHCl_3$). After evaporating the solvent, a dark red oil was obtained (56% yield). ^1H NMR (500 MHz, $CDCl_3$, 25 °C): δ (ppm) 9.13 (t; 2H; α-H), 8.55 (dd; 1H; α-H), 8.26 (dt; 2H; β-H), 7.67 (dd; 2H; γ-H), 7.64 (d; 1H; β-H), 7.51 (d; 1H; β-H), 7.17 (td; 1H; γ-H), 3.96 (s; 4H; CH_2), 3.94 (s; 6H; OCH_3), 3.90 (s; 2H; CH_2).

The syntheses of the mononuclear Fe^{II} complexes **3**−**6** and **9** were carried out under Ar by mixing equal molar amounts of $Fe^{II}(ClO_4)_2\cdot 6H_2O$ and the corresponding ligand in acetonitrile solution. The solid was obtained by diffusion of diethyl ether or di(isopropyl) ether into the acetonitrile solution. Complex **8** was synthesized by mixing equal molar amounts of $Fe^{II}(OTf)_2\cdot 2CH_3CN$ (OTf = trifluoromethanesulfonate) and BPQA in THF solution while stirring under Ar. After the solvent was evaporated, the residue was dissolved in CH_2Cl_2 and layered with hexane to afford a yellow solid upon standing at −20 °C for 3 days. All complexes gave satisfactory elemental analyses. Elemental analyses were performed at Atlantic Microlab (Norcross, GA) or M-H-W Laboratories (Phoenix, AZ). Crystals suitable for crystallographic analysis were obtained from CH_3CN/hexane for $[Fe^{II}(5\text{-}Me_3\text{-}TPA)(CH_3CN)_2](ClO_4)_2$ (**3**), CH_3CN/THF for $[Fe^{II}(3\text{-}Me_3\text{-}TPA)(CH_3CN)_2](ClO_4)_2$ (**4**), CH_2Cl_2/hexane for $[Fe^{II}(BPQA)(OTf)_2]$ (**8**), and $[Fe^{II}(BQPA)(H_2O)(ClO_4)](ClO_4)$ (**9**). *Caution: Perchlorate salts are potentially explosive and should be handled with care.*

$[Fe^{II}(5\text{-}Me_3\text{-}TPA)(CH_3CN)_2](ClO_4)_2$ (3). ^1H NMR (300 MHz, CD_3CN, 25 °C): δ (ppm) 10.8 (3H; α-H), 8.4 (3H; β-H), 7.1 (3H; γ-H), 6.2 (6H; CH_2), 2.2 (9H; CH_3). Anal. Calcd (found) for $C_{25}H_{30}N_6FeCl_2O_8$: C, 44.86 (44.81); H, 4.52 (4.50); N, 12.56 (12.42); Cl, 10.59 (10.73).

$[Fe^{II}(3\text{-}Me_3\text{-}TPA)(CH_3CN)_2](ClO_4)_2$ (4). ^1H NMR (300 MHz, CD_3CN, 25 °C): δ (ppm) 9.18 (3H; α-H), 7.53 (3H; β-H), 7.51 (3H; γ-H), 5.04 (6H; CH_2), 1.99 (9H; CH_3). Anal. Calcd (found) for $C_{25}H_{32}N_6FeCl_2O_9$ (**4**$\cdot H_2O$): C, 43.70 (44.03); H, 4.69 (4.63); N, 12.23 (12.22); Cl, 10.32 (10.34).

$[Fe^{II}(5\text{-}(MeOOC)\text{-}TPA)(CH_3CN)_2](ClO_4)_2$ (5): ^1H NMR (300 MHz, CD_3CN, 25 °C): δ (ppm) 11.51 and 11.04 (3H; α-H), 8.59, 8.56, and 8.48 (5H; β-H), 7.88 and 7.34 (3H; γ-H), 6.49, 6.41, and 6.29 (6H; CH_2), 3.88 (3H; OCH_3). Anal. Calcd (found) for $C_{26}H_{30}N_7FeCl_2O_{10.5}$ (**5**$\cdot CH_3CN\cdot 0.5H_2O$): C, 42.47 (42.93); H, 4.11 (4.09); N, 13.33 (13.11); Cl, 9.64 (9.22).

$[Fe^{II}(5\text{-}(MeOOC)_2\text{-}TPA)(CH_3CN)(H_2O)](ClO_4)_2$ (6): ^1H NMR (300 MHz, CD_3CN, 25 °C): δ (ppm) 12.4 and 11.9 (3H; α-H), 9.05 and 8.89 (4H; β-H), 7.79 and 7.21 (3H; γ-H), 7.21 and 6.89 (6H; CH_2), 3.85 (6H; OCH_3). Anal. Calcd (found) for $C_{24}H_{27}N_5FeCl_2O_{13}$: C, 40.02 (40.41); H, 3.78 (4.04); N, 9.72 (9.69); Cl, 9.84 (9.60).

$[Fe^{II}(BPQA)(OTf)_2]$ (8). ^1H NMR (300 MHz, CD_3CN, 25 °C): δ (ppm) 101.9 (2H; pyr α-H), 85.9 and 74.1 (4H; pyr CH_2), 50.4 and 47.0 (4H; pyr β-H), 50.0 (1H; quin 3-H), 35.6 (2H; quin CH_2), 18.6 (1H; quin 7-H), −0.80 (1H; quin 4-H), −2.46 (2H; pyr γ-H), −3.41 (1H; quin 5-H), −58.0 (2H; quin 6-H and 8-H). Anal. Calcd (found) for $C_{24}H_{22}N_4FeF_6O_7S_2$ (**8**$\cdot H_2O$): C, 40.46 (40.84); H, 3.11 (2.99); N, 7.86 (7.90); S, 9.00 (9.07).

$[Fe^{II}(BQPA)(H_2O)(ClO_4)](ClO_4)$ (9). ^1H NMR (300 MHz, CD_3CN, 25 °C): δ (ppm) 111.1 (1H; pyr α-H), 102.6 (2H; pyr CH_2), 65.4 (4H; quin CH_2), 58.9 and 51.7 (2H; pyr β-H), 56.1 (2H; quin 3-H),

(13) Groves, J. T.; Haushalter, R. C.; Nakamura, M.; Nemo, T. E.; Evans, B. J. *J. Am. Chem. Soc.* **1981**, *103*, 2884−2886.
(14) Kim, C.; Chen, K.; Kim, J.; Que, L., Jr. *J. Am. Chem. Soc.* **1997**, *119*, 5964−5965.
(15) Chen, K.; Que, L., Jr. *Chem. Commun.* **1999**, 1375−1376.
(16) Sono, M.; Roach, M. P.; Coulter, E. D.; Dawson, J. H. *Chem. Rev.* **1996**, *96*, 2842−2888.
(17) Dong, Y.; Fujii, H.; Hendrich, M. P.; Leising, R. A.; Pan, G.; Randall, C. R.; Wilkinson, E. C.; Zang, Y.; Que, L., Jr.; Fox, B. G.; Kauffmann, K.; Münck, E. *J. Am. Chem. Soc.* **1995**, *117*, 2778−2792.
(18) Nanthakumar, A.; Fox, S.; Murthy, N. N.; Karlin, K. D. *J. Am. Chem. Soc.* **1997**, *119*, 3898−3906.
(19) Tyeklár, Z.; Jacobson, R. R.; Wei, N.; Murthy, N. N.; Zubieta, J.; Karlin, K. D. *J. Am. Chem. Soc.* **1993**, *115*, 2677−2689.
(20) Wei, N.; Murthy, N. N.; Chen, Q.; Karlin, K. D. *Inorg. Chem.* **1994**, *33*, 1953−1965.
(21) Zang, Y.; Kim, J.; Dong, Y.; Wilkinson, E. C.; Appelman, E. H.; Que, L., Jr. *J. Am. Chem. Soc.* **1997**, *119*, 4197−4205.
(22) Lubben, M.; Meetsma, A.; Wilkinson, E. C.; Feringa, B.; Que, L., Jr. *Angew. Chem., Int. Ed. Engl.* **1995**, *34*, 1512−1514.
(23) (a) Kojima, T.; Leising, R. A.; Yan, S.; Que, L., Jr. *J. Am. Chem. Soc.* **1993**, *115*, 11328−11335. (b) Norman, R. E.; Yan, S.; Que, L., Jr.; Sanders-Loehr, J.; Backes, G.; Ling, J.; Zhang, J. H.; O'Connor, C. J. *J. Am. Chem. Soc.* **1990**, *112*, 1554−1562.

Table 1. Crystallographic Data of **3**, **4**, **8**, and **9**

	3	**4**·0.5CH_3CN	**8**	**9**
empirical formula	$C_{25}H_{30}Cl_2FeN_6O_8$	$C_{26}H_{31.5}Cl_2FeN_{6.5}O_8$	$C_{24}H_{20}F_6FeN_4O_6S_2$	$C_{26}H_{24}Cl_2FeN_4O_9$
formula weight	669.30	689.83	694.41	663.24
T	173(2) K	173(2) K	293(2) K	173(2) K
crystal system	triclinic	triclinic	trigonal	monoclinic
space group	*P*1	$P\bar{1}$	$P3_2$	$P2_1/n$
unit cell dimensions	$a = 8.5581(3)$ Å $b = 9.8036(3)$ Å $c = 10.6673(4)$ Å $\alpha = 64.651(1)°$ $\beta = 68.683(1)°$ $\gamma = 87.560(1)°$	$a = 11.468(2)$ Å $b = 11.835(2)$ Å $c = 12.691(2)$ Å $\alpha = 74.252(3)°$ $\beta = 77.657(3)°$ $\gamma = 68.165(3)°$	$a = 9.864(2)$ Å $b = 9.864(2)$ Å $c = 24.777(9)$ Å $\gamma = 120°$	$a = 10.0336(2)$ Å $b = 16.0283(4)$ Å $c = 17.3444(2)$ Å $\beta = 101.619(1)°$
V	746.65(7) Å^3	1526.5(5) Å^3	2088(1) Å^3	2732.19(9) Å^3
Z	1	2	3	4
D (calc)	1.489 g cm^{-3}	1.501 g cm^{-3}	1.657 g cm^{-3}	1.612 g cm^{-3}
λ	0.71073 Å	0.71073 Å	0.71073 Å	0.71073 Å
μ	0.741 mm^{-1}	0.727 mm^{-1}	0.779 mm^{-1}	0.810 mm^{-1}
R_1[a]	0.0245	0.0426	0.0786	0.0614
wR_2[b]	0.0621	0.0710	0.2068	0.1215

[a] $R_1 = \sum||F_o| - |F_c||/\sum|F_o|$. [b] $wR_2 = (\sum[w(F_o^2 - F_c^2)^2]/\sum[wF_o^4])^{1/2}$, where $w = q/\sigma^2(F_o^2) + (aP)^2 + bP$.

21.6 (2H; quin 7-H), 7.9 (2H; quin 5-H), −3.2 (2H; quin 6-H), −5.3 (2H; quin 4-H), −12.1 (1H; pyr γ-H), −53.7 (2H; quin 8-H). Anal. Calcd (found) for $C_{28}H_{29}N_5FeCl_2O_{10}$ (**9**·CH_3CN·H_2O): C, 46.56 (46.33); H, 4.05 (4.24); N, 9.70 (9.88).

The [Fe^{III}(L)Cl_2](ClO_4) complexes were obtained by combining equal molar amounts of $FeCl_3$·$6H_2O$, the ligand, and $NaClO_4$ in CH_3OH. Yellow crystals of **3b** (L = 5-Me_3-TPA) and **4b** (L = 3-Me_3-TPA) were obtained upon storing the solutions at 4 °C overnight. Orange-red crystals of **5b** (L = 5-(MeOOC)-TPA) and **6b** (L = 5-$(MeOOC)_2$-TPA) were obtained by vapor diffusion of diethyl ether into the methanol solutions at 4 °C. All complexes gave satisfactory elemental analyses (Atlantic Microlab, Norcross, GA).

[Fe^{III}(5-Me_3-TPA)Cl_2](ClO_4) (3b). ^{1}H NMR (300 MHz, CD_3CN, 25 °C): δ (ppm) 168, 120, 106, 14, 9.6, −0.5. Anal. Calcd (found) for $C_{21}H_{24}N_4FeCl_3O_4$: C, 45.15 (45.20); H, 4.33 (4.31); N, 10.03 (9.96); Cl, 19.04 (19.17).

[Fe^{III}(3-Me_3-TPA)Cl_2](ClO_4) (4b). ^{1}H NMR (300 MHz, CD_3CN, 25 °C): δ (ppm) 146, 120, 7.2, 5.1, 0.38, 0.20. Anal. Calcd (found) for $C_{21}H_{24}N_4FeCl_3O_4$: C, 45.15 (44.71); H, 4.33 (4.34); N, 10.03 (9.87); Cl, 19.04 (18.87).

[Fe^{III}(5-(MeOOC)-TPA)Cl_2](ClO_4) (5b). ^{1}H NMR (300 MHz, CD_3CN, 25 °C): δ (ppm) 142, 116, 94, 46, 4.4, 3.8. Anal. Calcd (found) for $C_{20}H_{20}N_4FeCl_3O_6$: C, 41.80 (41.94); H, 3.51 (3.95); N, 9.75 (9.23); Cl, 18.51 (18.82).

[Fe^{III}(5-$(MeOOC)_2$-TPA)Cl_2](ClO_4) (6b). ^{1}H NMR (300 MHz, CD_3CN, 25 °C): δ (ppm) 140, 117, 110, 95, 7.4, 4.4. Anal. Calcd (found) for $C_{24}H_{27}N_4FeCl_3O_{8.5}$ (**6b**·$0.5C_4H_{10}O$): C, 43.04 (43.05); H, 4.06 (3.82); N, 8.37 (8.53).

Instrumentation. ^{1}H NMR spectra were recorded on Varian Unity 300 and 500 spectrometers at ambient temperature. Chemical shifts (ppm) were referenced to the residual protic solvent peaks.

Electrochemical studies were carried out with a CS-100 electrochemical analyzer (Cypress Systems, Inc., Lawrence, KS) using 0.1 M NBu_4BF_4 in acetonitrile as the supporting electrolyte. Cyclic voltammograms (CV) were obtained with a scan rate of 100 mV s^{-1} by using a three-component system consisting of a platinum disk working electrode and silver wires as auxiliary and reference electrodes. Potentials were corrected to the SCE standard by using [Fe^{II}(bipy)$_3$](ClO_4)$_2$[24] as the internal standard ($E_{1/2}$ ($Fc^{+1/0}$) = 380 mV under the same conditions). All waves were quasi-reversible with ΔE's of less than 84 mV.

Crystallographic analyses were conducted at the X-ray Crystallographic Laboratory of the Chemistry Department of the University of Minnesota. Data were collected on a Siemens SMART system as previously reported.[21] Pertinent crystallographic data and experimental conditions are summarized in Table 1. The structures were solved by direct methods using the SHELXTL V5.0 suite of programs. All non-hydrogen atoms were refined anisotropically, and hydrogen atoms were placed in ideal positions and refined as riding atoms with individual (or group if appropriate) isotropic displacement parameters.

Product analyses were performed on a Perkin-Elmer Sigma 3 gas chromatography (AT-1701 column, 30 m) and a flame-ionization detector. GC mass spectral analyses were performed on a HP 5898 GC (DB-5 column, 60 m) with a Finnigan MAT 95 mass detector or a HP 6890 GC (HP-5 column, 30 m) with an Agilent 5973 mass detector. NH_3/CH_4 (4%) was used as the ionization gas for chemical ionization analyses.

Reaction Conditions. In a typical reaction, 0.3 mL of a 70 mM H_2O_2 solution (diluted from 35% or 50% H_2O_2/H_2O solution) in CH_3CN was delivered by syringe pump over 30 min at 25 °C in air to a vigorously stirred CH_3CN solution (2.7 mL) containing iron catalyst and alkane substrate. The final concentrations of reagents were 0.70 mM mononuclear iron catalyst **1**−**11** or 0.35 mM diiron catalyst **1a**, 7.0 mM H_2O_2, and 0.70 M cyclohexane, *cis*- or *trans*-1,2-dimethylcyclohexane, 70 mM *cis*- or *trans*-decalin, or 7.0 mM adamantane. The solution was stirred for another 5 min after syringe pump addition. The iron complex was removed by passing the solution through silica gel followed by elution with 3 mL of CH_3CN. An internal standard was added at this point, and the solution was subjected to GC analysis. The organic products were identified by GC−MS comparison with authentic compounds. In the studies of kinetic isotope effects, a substrate mixture of cyclohexane/cyclohexane-d_{12} of 1:2 or 1:3 was used to improve the accuracy of the KIE values obtained. All reactions were run at least in triplicate, and the data reported was the average of these reactions.

Isotope-Labeling Studies. Similar conditions as described above were used for isotope-labeling studies except for the following details. In experiments with $H_2{}^{18}O$, 42 μL of $H_2{}^{18}O$ (0.70 M) was added to the catalyst solution prior to the addition of H_2O_2. In experiments with $H_2{}^{18}O_2$, 7.0 mM $H_2{}^{18}O_2$ (diluted by CH_3CN from a 2% $H_2{}^{18}O_2/H_2O$ solution) was used instead of H_2O_2. In experiments with $^{18}O_2$, both the catalyst and alkane mixture and the H_2O_2 solution were degassed by four freeze-vacuum-thaw cycles prior to the reaction being performed under an $^{18}O_2$ atmosphere. The product solution in the oxidation of *cis*-1,2-dimethylcyclohexane or adamantane was passed through silica gel, while other reaction solutions were treated with 0.1 mL of 1-methylimidazole and 1 mL of acetic anhydride to esterify the alcohol products[25] (*cis*-1,2-dimethylcyclohexanol was not esterified under the experimental conditions) for GC−MS analyses. A substrate mixture of 0.35 M cyclohexane-d_{12} and 0.35 M cyclohexane or 0.35 M cyclohexane-d_{12} and 0.35 M cyclooctane was used to study intermolecular C−H/D bond-dependent ^{18}O-incorporation, while 0.70 M *cis*- or *trans*-1,2-dimethylcyclohexane or 7.0 mM adamantane was used

(24) Burstall, F. H.; Nyholm, R. S. *J. Chem. Soc.* **1952**, 3570−3579.

(25) Elvebak, L. E., II.; Schmitt, T.; Gray, G. R. *Carbohydr. Res.* **1993**, *246*, 1−11.

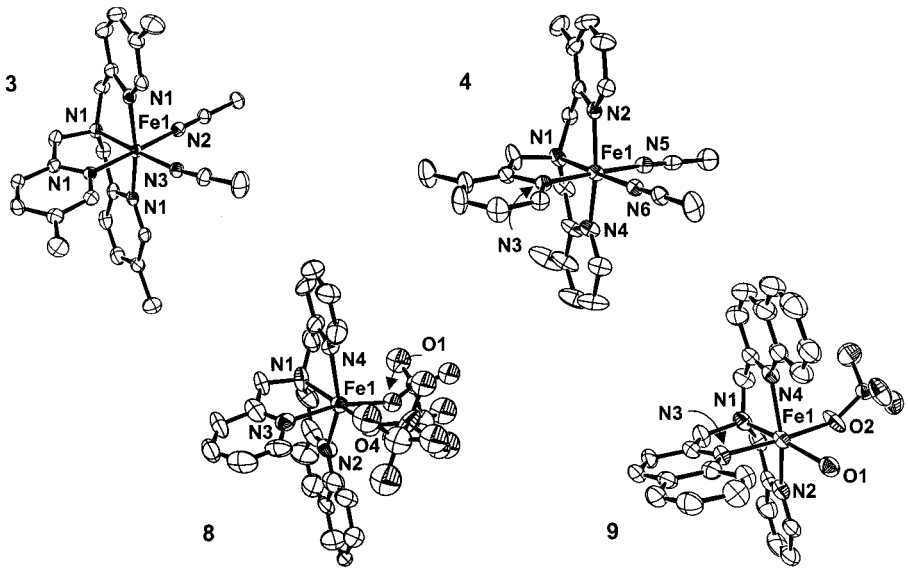

Figure 1. ORTEP plots of $[Fe^{II}(5\text{-}Me_3\text{-}TPA)(CH_3CN)_2]^{2+}$ (**3**), $[Fe^{II}(3\text{-}Me_3\text{-}TPA)(CH_3CN)_2]^{2+}$ (**4**), $[Fe^{II}(BPQA)(OTf)_2]$ (**8**), and $[Fe^{II}(BQPA)(H_2O)(ClO_4)]^+$ (**9**). Ellipsoids are drawn at the 50% probability level. Hydrogen atoms are omitted for clarity.

separately for other C−H bond-dependent ^{18}O-incorporation experiments. The ^{16}O and ^{18}O compositions of the alcohol products were determined by the relative abundances of the following peaks: cyclohexanol (CI), $m/z = 160$ (^{16}O) and 162 (^{18}O); cyclohexanol-d_{11} (CI), $m/z = 171$ (^{16}O) and 173 (^{18}O); cyclooctanol (CI), $m/z = 188$ (^{16}O) and 190 (^{18}O); 1-adamantanol (CI), $m/z = 170$ (^{16}O) and 172 (^{18}O); (*cis* or 1*R*,2*R*/1*S*,2*S*)-1,2-dimethylcyclohexanol (CI), $m/z = 146$ (^{16}O) and 148 (^{18}O); the secondary alcohols in the oxidation of *trans*-1,2-dimethylcyclohexane (CI), $m/z = 188$ (^{16}O) and 190 (^{18}O); (*trans* or 1*R*,2*S*/1*S*,2*R*)-1,2-dimethylcyclohexanol (EI), the average of $m/z = 128$ (^{16}O) and 130 (^{18}O), 113 (^{16}O) and 115 (^{18}O), 85 (^{16}O) and 87 (^{18}O), 71 (^{16}O) and 73 (^{18}O). All reactions were run at least in triplicate. The data reported was the average of these reactions and calculated based on the ^{18}O-enrichment of the reagents containing the isotope.

Table 2. Selected Bond Lengths (Å) and Angles (deg) in $[Fe^{II}((TPA)(CH_3CN)_2]^{2+}$ (1), $[Fe^{II}(5\text{-}Me_3\text{-}TPA)(CH_3CN)_2]^{2+}$ (**3**), $[Fe^{II}(3\text{-}Me_3\text{-}TPA)(CH_3CN)_2]^{2+}$ (**4**), $[Fe^{II}(BPQA)(OTf)_2]$ (**8**), $[Fe^{II}((BQPA)(H_2O)(ClO_4)]^+$ (**9**), and $[Fe^{II}(6\text{-}Me_3\text{-}TPA)(CH_3CN)_2]^{2+}$ (**11**)

	1[21]	**3**	**4**	**8**	**9**	**11**[21]
$Fe-N_{amine}$	1.99	1.998(3)	1.972(2)	2.208(9)	2.197(4)	2.15
$Fe-N_{aromatic}$	1.97	1.984(3)	1.973(3)	2.267(8)	2.184(4)	2.25
	1.92	1.969(3)	1.955(3)	2.138(9)	2.172(4)	2.18
	1.95	1.985(3)	1.962(3)	2.196(8)	2.201(4)	2.24
$Fe-N_{acetonitrile}$	1.92	1.960(3)	1.947(3)	−	−	2.17
	1.93	1.948(3)	1.933(3)			2.17
$Fe-O_{other\ ligand}$	−	−	−	2.056(18)	2.094(3)	−
				2.172(13)	2.262(3)	

Results and Discussion

A Family of Fe^{II}(TPA) Complexes. $[Fe^{II}(TPA)(CH_3CN)_2]^{2+}$ (**1**), where TPA is the tetradentate tripodal tris(2-pyridylmethyl)-amine ligand (Scheme 1), is the first non-heme iron catalyst reported capable of stereospecific alkane hydroxylation in combination with H_2O_2.[14] Subsequently, we have found that the same transformation is also catalyzed by the closely related $[Fe^{II}(BPMEN)(CH_3CN)_2]^{2+}$ (**2**), where BPMEN is the linear tetradentate *N*,*N*′-dimethyl-*N*,*N*′-bis(2-pyridylmethyl)-1,2-diaminoethane ligand (Scheme 1).[15] Since various substituents can be readily introduced into the pyridyl rings (Scheme 1), the TPA ligand is flexible enough to allow a systematic study of ligand electronic and steric effects on the properties and reactivities of the iron complex. The series of iron(II) complexes we have synthesized for this effort can be formulated as $[Fe^{II}(L)XY]$, where L is the tetradentate ligand and the two *cis*-oriented monodentate ligands X and Y may be solvent molecules such as CH_3CN and H_2O or anions such as ClO_4^- and triflate (OTf^-) (Figure 1).

The family of Fe^{II}(TPA) complexes can be divided into two categories. One group consists of Fe^{II}(TPA) complexes wherein pyridyl β-Hs are replaced by different functional groups (**3**−**6**, Scheme 1). As found for **1**,[21] the Fe^{II} center is in the diamagnetic low-spin state as shown by the <2 Å Fe−N distances found in crystal structures of **3** and **4** (Table 2 and Figure 1) and the compact NMR shift range of 0−12 ppm (Figure 2). The NMR shifts are modulated by the electronic properties of the substituents; **5** and **6** exhibit more downfield shifted NMR features than **3** and **4** (Figure 2), in line with the increased Lewis acidity of the iron center on going from −Me to −COOMe groups. The electronic effects of β-substituents can also be observed in electrochemical studies of the corresponding $[Fe^{III}(L)Cl_2](ClO_4)$ complexes. The $E_{1/2}(Fe^{3+}/Fe^{2+})$ value decreases as the electron donating ability of the ligand is increased, that is, 5-$(MeOOC)_2$-TPA < 5-(MeOOC)-TPA < TPA < 5-Me_3-TPA ≈ 3-Me_3-TPA (Figure 2). These results show that the higher iron oxidation state is stabilized by electron donating β-substituents on the TPA ligand.

The second group consists of complexes of TPA ligands with α-substituents (**7**−**11**, Scheme 1). As noted previously, substituents at the pyridyl α-position introduce steric effects on the metal center that prevent the pyridyl groups from approaching the iron center too closely.[21,26−28] Consequently, the α-substituted TPA ligands favor metal centers with larger ionic radii, for example, Fe^{II} over Fe^{III}, high-spin over low-spin. Indeed, complexes **7**−**11** all have high-spin Fe^{II} centers, as indicated by ^1H NMR shifts of up to 160 ppm. As previously reported for **11**,[21] the crystal structures of **8** and **9** have an average $Fe-N_{TPA}$ distance of 2.20 Å (Table 2 and Figure 1), distances typical of high-spin Fe^{II} centers. We have thus obtained

(26) Gütlich, P. *Struct. Bonding* **1981**, *44*, 83−195.
(27) Gütlich, P.; Hauser, A.; Spiering, H. *Angew. Chem., Int. Ed. Engl.* **1994**, *33*, 2024−2054.
(28) Constable, E. C.; Baum, G.; Bill, E.; Dyson, R.; van Eldik, R.; Fenske, D.; Kaderli, S.; Morris, D.; Neubrand, A.; Neuburger, M.; Smith, D. R.; Wieghardt, K.; Zehnder, M.; Zuberbühler, A. D. *Chem. Eur. J.* **1999**, *5*, 498−508.

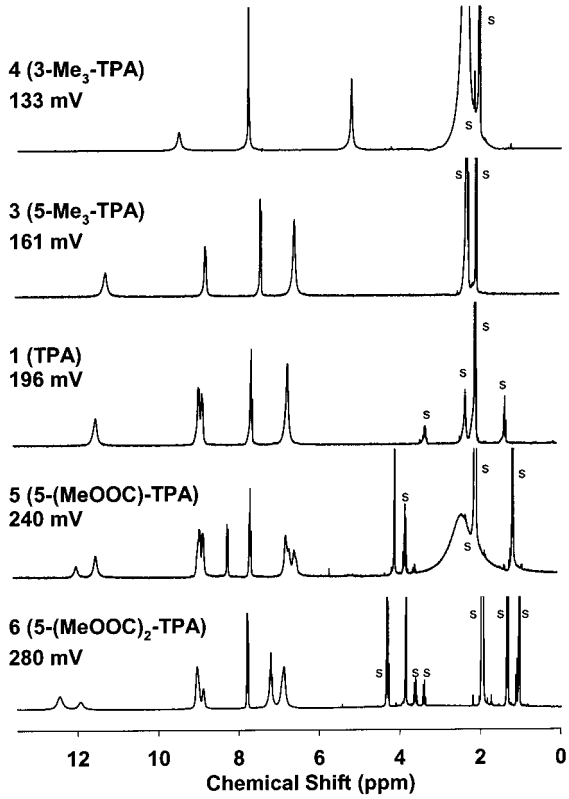

Figure 2. ^{1}H NMR spectra of complexes **1** and **3**−**6** in CD_3CN at room temperature with $E_{1/2}$ (Fe^{3+}/Fe^{2+}) values of the corresponding $[Fe^{III}LCl_2]^+$ complexes (**1b** and **3b**−**6b**). Residual solvent peaks are labeled "s".

a family of Fe^{II}(TPA) complexes that can be used to study ligand tuning effects on their ability to catalyze alkane hydroxylation. These studies are discussed in the next section.

Reactivity Patterns for Alkane Hydroxylation. In a typical reaction, 0.70 mM **1** is treated with 7.0 mM H_2O_2 (10 equiv) in the presence of 0.70 M cyclohexane (1000 equiv) in acetonitrile at room temperature in air. The oxidant is delivered by syringe pump over a 30-min period to suppress H_2O_2 disproportionation and enhance its conversion to organic products.[29] All of the oxidant is consumed at the end of the reaction as indicated by iodometry. While no products are observed in the reaction of cyclohexane and H_2O_2 in the absence of catalyst, 2.7 TN cyclohexanol (A) and 0.5 TN cyclohexanone (K) are obtained in the presence of **1**. This result corresponds to a 32% conversion of the oxidant into organic products. Essentially the same product distribution is obtained under Ar, demonstrating that O_2 does not play a significant role in the reaction. In support, less than 3(2)% ^{18}O is incorporated from $^{18}O_2$ into the cyclohexanol product when **1**-catalyzed oxidation is carried out under an $^{18}O_2$ atmosphere. Significantly, the percent conversion of H_2O_2 into alkane oxidation products remains the same with subsequently repeated additions of oxidant into the mixture of the catalyst and the alkane substrate (Figure 3b). Its high efficiency and robust nature as well as the short reaction time required for reaction make **1** among the best non-heme iron catalysts reported for alkane hydroxylation with H_2O_2.[12]

The alkane hydroxylation reactivity patterns observed for **2**−**6** are very similar to that found for **1** (Table 3). First of all, the alcohol accounts for >80% of the products in the oxidation of cyclohexane. The A/K ratio is unaffected by the presence of

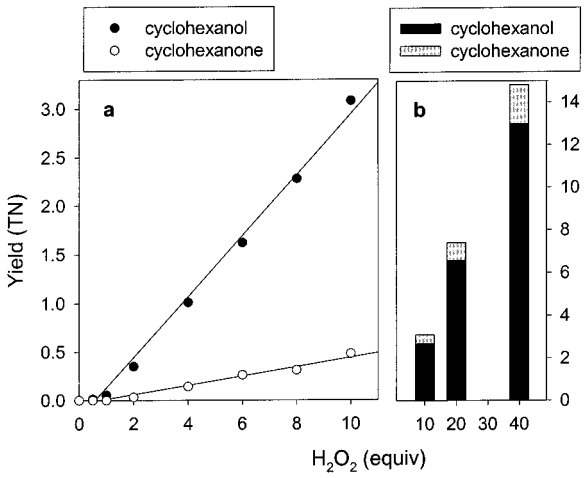

Figure 3. Product yields as a function of equivalents of H_2O_2 added into the acetonitrile solution of **1** and 1000 equiv of cyclohexane in air: (a) 0−10 equiv of H_2O_2; (b) 10−40 equiv of H_2O_2.

O_2, showing that the cleavage of alkane C−H bonds does not generate long-lived alkyl radicals that are susceptible to radical chain autoxidation. Second, the results of competitive oxidations of C−H bonds of different strengths indicate the involvement of a rather selective oxidant. For example, intermolecular kinetic isotope effects (KIE) of 3.2−3.8 are observed for cyclohexanol formation and 3°/2° ratios of 15−27 are found in the oxidation of tertiary and secondary C−H bonds of adamantane. Third and most significantly, **1**−**6** can catalyze stereospecific alkane hydroxylation. For example, the oxidation of *cis*-1,2-dimethylcyclohexane gives as the major product (1*R*,2*R* or 1*S*,2*S*)-1,2-dimethylcyclohexanol, the tertiary alcohol with the methyl groups *cis* to each other, and its epimer is not observed. The only tertiary alcohol product in corresponding experiments with *trans*-1,2-dimethylcyclohexane substrate is (1*R*,2*S* or 1*S*,2*R*)-1,2-dimethylcyclohexanol, the epimer with the methyl groups *trans* to each other (Table S1). Thus hydroxylation proceeds with retention of configuration at C-1. The same stereospecificity is also observed in the **1**-catalyzed hydroxylation of the tertiary C−H bonds of *cis*- or *trans*-decalin. This reactivity pattern in fact resembles that associated with iron porphyrin catalysts (Table 3).[30−33] Thus, **1**−**6** are quite selective catalysts for alkane hydroxylation with H_2O_2.

The reactivity patterns of **1**−**6** significantly differ from other non-heme iron catalysts reported in the literature.[12] Most non-heme iron/H_2O_2 reactions generate HO• that reacts with alkanes to afford long-lived alkyl radicals as indicated by four symptoms (Table 3):[35−37,39] (1) an A/K ratio ≈ 1; (2) the sensitivity of the product distribution to the presence of O_2, with the oxygen atom in the alcohol product deriving from O_2; (3) low selectivity in

(29) Kim, J.; Harrison, R. G.; Kim, C.; Que, L., Jr. *J. Am. Chem. Soc.* **1996**, *118*, 4373−4379.
(30) Groves, J. T.; Nemo, T. E. *J. Am. Chem. Soc.* **1983**, *105*, 6243−6248.
(31) Khenkin, A. M.; Shilov, A. E. *New J. Chem.* **1989**, *13*, 659−667.
(32) Sorokin, A. B.; Khenkin, A. M. *New J. Chem.* **1990**, *14*, 63−67.
(33) Dores Assis, M.; Lindsay Smith, J. R. *J. Chem. Soc., Perkin Trans. 2* **1998**, 2221−2226.
(34) Mekmouche, Y.; Duboc-Toia, C.; Ménage, S.; Lambeaux, C.; Fontecave, M. *J. Mol. Catal. A: Chem.* **2000**, *156*, 85−89.
(35) Trotman-Dickenson, A. F. *Adv. Free Radical Chem.* **1965**, *1*, 1−38.
(36) Buxton, G. V.; Greenstock, C. L.; Helman, W. P.; Ross, A. B. *J. Phys. Chem. Ref. Data* **1988**, *17*, 513−886.
(37) Miyajima, S.; Simamura, O. *Bull. Chem. Soc. Jpn.* **1975**, *48*, 526−530.
(38) Roelfes, G.; Lubben, M.; Hage, R.; Que, L., Jr.; Feringa, B. L. *Chem. Eur. J.* **2000**, *6*, 2152−2159.
(39) Ingold, K. U.; MacFaul, P. A. In *Biomimetic Oxidations Catalyzed by Transition Metal Complexes*; Meunier, B., Ed.; World Scientific Publishing and Imperial College Press: London, 2000; Chapter 2.

Table 3. Oxidation of Alkanes with H_2O_2 Catalyzed by **1**−**11**[a] and Other Catalysts

		cyclohexane			*cis*−1,2-dimethylcyclohexane		adamantane
$Fe^{II}L$	L	A + K[b]	A/K	KIE[c]	3°-ol[b]	RC[d] (%)	3°/2° [e]
1	TPA	3.2(6)	5	3.5[14]	3.8(9)	100	17
2	BPMEN	6.3(5)	8	3.2(1)	4.6(1)	96	15
3	5-Me_3-TPA	4.0(5)	9	3.8(1)	3.6(1)	100	21
4	3-Me_3-TPA	4.5(5)	14	3.7(6)	4.5(1)	100	27
5	5-(MeOOC)-TPA	4.0(1)	5	- - -	4.1(2)	100	- - -
6	5-$(MeOOC)_2$-TPA	2.3(6)	19	3.7(5)	3.4(2)	100	15
7	6-Me-TPA	4.0(4)	7	3.6(3)	2.4(3)	85	30
8	BPQA	5.8(2)	10	3.4(1)	3.4(3)	89	30
9	BQPA	1.7(1)	2	3.5(1)	2.0(2)	74	27
10	6-Me_2-TPA	2.9(2)	2	4.0(8)	1.8(1)	64	33
11	6-Me_3-TPA	1.4(3)	1	3.3(1)	1.0(3)	54	15
	$[Fe^{III}_2(O)(TPA)_2(H_2O)_2]^{4+}$ (**1a**)	4.3(4)	5				
	$[Fe^{III}_2(O)(pb)_4(H_2O)_2]^{4+}$ [f] (ref 34)		2.6	3.2		100	3.5
	$Fe^{II}(ClO_4)_2$					23	
	HO• (refs 35−37)		1	1−2		9	2
	$[Fe^{II}(N4Py)(CH_3CN)]^{2+}$ (**12**)[g] (ref 38)		1.4	1.5		27	3.3
	$Fe^{III}(Por)$[f,h] (refs 30−33)		5−15	13		96	6−48

[a] Iron catalyst:H_2O_2:alkane = 1:10:1000 for cyclohexane and *cis*-1,2-dimethylcyclohexane or 1:10:10 for adamantane oxidation by syringe pump in acetonitrile in air. [b] Turnover number (TN, mole of product/mole of iron), A = cyclohexanol, K = cyclohexanone, 3°-ol = all isomers of 1,2-dimethylcyclohexanol. [c] KIE = intermolecular kinetic isotope effect of cyclohexanol formation. [d] RC = retention of configuration in the oxidation of the tertiary C−H bonds of *cis*-1,2-dimethylcyclohexane, expressed as the ratio of the tertiary alcohols: [(1*R*,2*R* + 1*S*,2*S*) − (1*R*,2*S* + 1*S*,2*R*)]/3°-ol. (Note: The tertiary alcohol obtained by C1-hydroxylation with retention of configuration, i.e., having the methyl groups *cis* to each other, is the 1*R*,2*R* or the 1*S*,2*S* isomer; it has been incorrectly called *cis*-1,2-dimethylcyclohexanol in the recent literature[14,15,45,64] but should actually be referred to as the *trans* isomer according to IUPAC rules. We thank a reviewer of this paper for pointing out this error.) [e] 3°/2°= (1-adamantanol)/(2-adamantanol + 2-adamantanone) taking into account of the number of C−H bonds in a group. See Table S1 for product turnover data. [f] pb = (−)-4,5-pinenebipyridine. Por = porphinato dianion. [g] Under Ar. [h] With single-oxygen-atom donors such as PhIO or NaOCl.

C−H bond oxidation (such as a KIE value for cyclohexane oxidation of 1−2 or a 3°/2° ratio in adamantane oxidation of 2); (4) low stereoselectivity in the oxidation of *cis* or *trans* stereoisomers of 1,2-dimethylcyclohexane and decalin due to the epimerization of long-lived tertiary alkyl radicals (rate constant estimated to be 10^8−10^9 s^{-1}).[31,37,40,41] In fact, with Fenton's reagent such as $Fe^{II}(ClO_4)_2/H_2O_2/H^+$ ($HClO_4$ or H_2SO_4)[42] under the same experimental conditions, (1*R*,2*R* + 1*S*,2*S*)/(1*R*,2*S* + 1*S*,2*R*) tertiary alcohol ratios of 1.6(1) and 1.2 are obtained in the oxidations of *cis*- and *trans*-1,2-dimethylcyclohexane, respectively. The reaction profiles exhibited by **1**−**6** clearly show that HO• is not involved; instead, they strongly suggest the involvement of a more selective metal-based oxidant that generates short-lived alkyl radicals.

The α-substituted subgroup of Fe^{II}(TPA) catalysts exhibits a different reactivity pattern (Table 3). For example, the A/K ratio decreases significantly in the oxidation of cyclohexane for the catalysts with more than one α-substituent. In the extreme case of **11**, nearly equal amounts of alcohol and ketone are formed. Moreover, O_2 plays a significant role in these reactions, as shown by the significant amounts of ^{18}O incorporated into the alcohol products when the reactions are performed under an $^{18}O_2$ atmosphere (Table 4). Furthermore, the hydroxylation of *cis*-1,2-dimethylcyclohexane by **7**−**11** affords the two epimeric tertiary alcohol products. Indeed, as illustrated in Figure 4, there appears to be a linear correlation between the increasing amount of ^{18}O-incorporation from $^{18}O_2$ into the cyclohexanol product and the loss of stereoselectivity in the hydroxylation of *cis*-1,2-dimethylcyclohexane when the Fe^{II}(TPA) catalysts have more α-substituents on the TPA ligand. These results indicate that alkane oxidations by **7**−**11** involve alkyl radicals with longer lifetimes than those that may be produced in the reactions of **1**−**6**.

Table 4. Percentage of ^{18}O-incorporation into Alcohol in the Oxidation of Cyclohexane by **1**−**11**[a]

$Fe^{II}L$	L	$H_2{}^{18}O$	$H_2{}^{18}O_2$	$^{18}O_2$
1	TPA	27(2)	70(5)	3(2)
2	BPMEN	18(3)	84(4)	0[b]
3	5-Me_3−TPA	38(1)	69(1)	0[b]
4	3-Me_3−TPA	30(2)	−	−
5	5-(MeOOC)-TPA	23(2)	−	−
6	5-$(MeOOC)_2$-TPA	19(1)	−	−
7	6-Me-TPA	14(4)	62(1)	25(3)
8	BPQA	7(1)	71(13)	22[b]
9	BQPA	0	56(6)	45(6)
10	6-Me_2-TPA	0	49(2)	54(6)
11	6-Me_3-TPA	1(1)	22(4)	77[b]

[a] Iron catalyst:H_2O_2:H_2O:cyclohexane = 1:10:1000:1000 by syringe pump in acetonitrile in the presence of isotopically labeled reagent. [b] Calculated based on the mass balance of oxygen derived from $H_2{}^{18}O$ and $H_2{}^{18}O_2$.

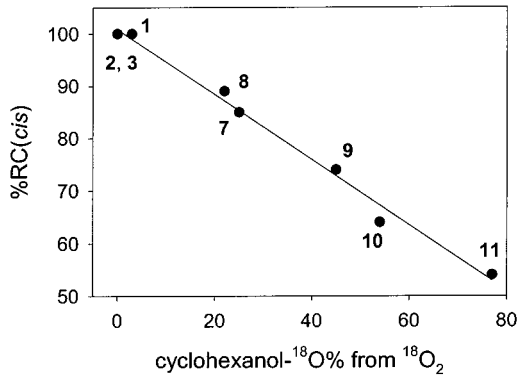

Figure 4. The linear correlation between the stereoselectivity in the hydroxylation of tertiary C−H bonds of *cis*-1,2-dimethylcyclohexane and ^{18}O-incorporation from $^{18}O_2$ into the alcohol product in the oxidation of cyclohexane by **1**−**3** and **7**−**11** (r^2 = 0.991).

The linear correlation in Figure 4 reflects the competition between the rebound of the nascent alkyl radical onto the metal center and either the epimerization of the tertiary *cis*-1,2-

(40) Bartlett, P. D.; Pincock, R. E.; Rolston, J. H.; Schindel, W. G.; Singer, L. A. *J. Am. Chem. Soc.* **1965**, *87*, 2590−2596.
(41) Krusic, P. J.; Meakin, P.; Jesson, J. P. *J. Phys. Chem.* **1971**, *75*, 3438−3453.
(42) Russell, G. A. *J. Am. Chem. Soc.* **1957**, *79*, 3871−3877.

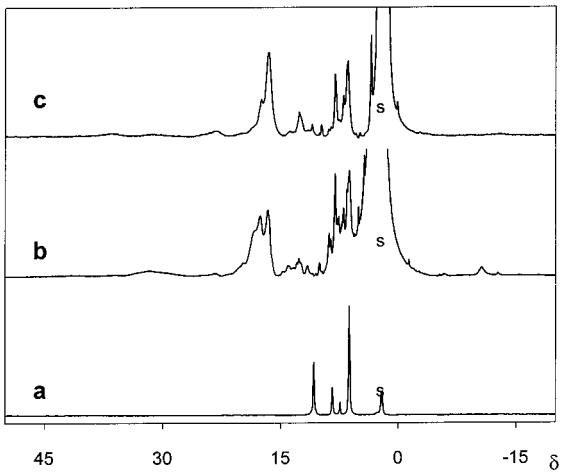

Figure 5. The NMR spectra of: (a) **1** in CD_3CN; (b) after the addition of 0.5 equiv of H_2O_2 by syringe pump into an CD_3CN solution of **1** and 1000 equiv of cyclohexane; and (c) after the addition of 10 equiv of H_2O_2 by syringe pump into an CD_3CN solution of **1** and 1000 equiv of cyclohexane.

dimethylcyclohexyl radical or the trapping of the cyclohexyl radical by O_2. The stereospecificity of **1**−**6** requires that the rate of radical rebound must be at least 2 orders of magnitude faster than the epimerization rate (10^8−10^9 s^{-1}),[31,41] and the nascent alkyl radicals must have lifetimes shorter than 10^{-10} s. Introduction of α-substituents in catalysts **7**−**11** presumably slows down the rebound step significantly and lengthens the lifetimes of alkyl radicals to the range of 10^{-9}−10^{-8} s, as calculated from their decreased stereoselectivities. This range of radical lifetimes is consistent with the amounts of ^{18}O-incorporation from $^{18}O_2$ in the oxidations of cyclohexane (O_2 trapping rate constant estimated to be about 3×10^7 s^{-1} under the experimental conditions).[43]

The longer-lived alkyl radicals formed in alkane oxidations by complexes **7**−**11**, however, do not derive from hydrogen abstraction by the nonselective HO•, as found for alkane hydroxylation by many other non-heme iron catalysts.[12] Complexes **7**−**11** all give rise to KIE values of 3−4 in the hydroxylation of cyclohexane/cyclohexane-d_{12} and 3°/2° ratios >15 in the oxidation of adamantane, values comparable to those found for complexes **1**−**6**. Therefore, a rather selective metal-based oxidant is still involved in the oxidation of C−H bonds by the α-substituted Fe^{II}(TPA) catalysts, and the longer radical lifetime very likely results from the steric effects of the α-substituents.

Participation of an Iron(III) Species. Detailed mechanistic studies on **1**-catalyzed alkane hydroxylation help to clarify the nature of the metal-based oxidant. When cyclohexane oxidation is monitored as a function of added H_2O_2, the amounts of alcohol and ketone products increase linearly with increasing amounts of H_2O_2 (Figure 3a). However, no organic product is detected upon the addition of the first 0.5 equiv H_2O_2 (Figure 3a), a result that is confirmed with the use of 10-fold higher amounts of the catalyst and H_2O_2 to improve the accuracy of the GC analysis. On the other hand, the addition of 0.5 equiv H_2O_2 to **1** changes its NMR spectrum dramatically (Figure 5), with the replacement of the sharp NMR features of diamagnetic **1** in the 0−11 ppm region with broader peaks spanning up to 40 ppm in shift, an NMR spectrum characteristic of an $Fe^{III}_2(\mu\text{-O})$ complex.[17] This broad NMR spectrum persists in samples studied at the end of the reaction with 10 equiv H_2O_2 (Figure 5). Therefore, it is likely that the first 0.5 equiv H_2O_2 oxidizes **1** to a mononuclear Fe^{III} species, which then converts to an oxo-bridged dimer, the thermodynamic sink for the Fe^{III} state.[44]

In support of this notion, we have found that $[Fe^{III}_2O(TPA)_2(H_2O)_2](ClO_4)_4$ (**1a**) has a catalytic efficiency comparable to that of **1** and affords a similar A/K ratio in the oxidation of cyclohexane. With 10 equiv H_2O_2, **1a** affords 3.6(4) TN cyclohexanol and 0.7(2) TN cyclohexanone under the same conditions as that for **1** (Table 3). However unlike **1,** there is no lag phase observed in product formation for **1a**. Indeed, the oxidation of cyclohexane by **1a** proceeds even when only 0.25 equiv of H_2O_2 per Fe is added, affording 0.064(2) TN cyclohexanol and <0.001(1) TN cyclohexanone (per Fe), a result confirmed by using 10-fold higher concentrations of the catalyst and H_2O_2. Thus, both **1** and **1a** act as precursors to the active oxidant for alkane hydroxylation.

The excellent catalytic efficiency of **1a** contrasts the reactivity of other Fe^{III}(TPA) complexes studied here, which are **not** catalysts for alkane hydroxylation. For example, no products are observed when $[Fe^{III}(TPA)Cl_2](ClO_4)$, $[Fe^{III}(TPA)Br_2](ClO_4)$, $[Fe^{III}_2O(TPA)_2(O_2CCH_3)](ClO_4)_3$, or $[Fe^{III}_2O(TPA)_2(O_2CPh)](ClO_4)_3$ is used as the catalyst under conditions that elicit cyclohexane oxidation by **1**−**11**. A similar ligand effect has been observed in a study by Mekmouche et al.[45] The differences in catalytic behavior in these studies emphasize an important element in catalyst design. In our study, only those complexes with solvent ligands or weakly coordinated anions are good catalysts that carry out alkane hydroxylation via a mechanism involving a metal-based oxidant. In our view, these weak ligands can be readily displaced by H_2O_2 to generate iron−peroxo species that are responsible for the novel metal-centered alkane hydroxylation chemistry reported in this paper.

Nature of the Metal-Based Oxidant. The reaction of **1** or **1a** with excess H_2O_2 generates an Fe^{III}−OOH intermediate, which has been successfully trapped at −40 °C and characterized by various spectroscopic techniques.[14,46] The Fe^{III}−OOH intermediate exhibits EPR signals at $g = 2.19$, 2.15, and 1.97, which can be associated with a low-spin iron(III) center and can be formulated as $[Fe(TPA)(OOH)]^{2+}$ by electrospray ionization mass spectrometry.[14] Addition of $H_2{}^{18}O$ does not affect its mass spectrum, demonstrating that the peroxo oxygens do not exchange with solvent $H_2{}^{18}O$.[47] Resonance Raman studies show features at 632 and 789 cm^{-1} that have been assigned to ν(Fe−OOH) and ν(O−O) modes, respectively.[46] These values suggest that the low-spin $[Fe^{III}(TPA)(OOH)]^{2+}$ intermediate has a stronger Fe−O bond and a weaker O−O bond relative to those of other iron−peroxo complexes.[46,48]

Subsequent reaction of this intermediate with alkane results in alkane hydroxylation, which may be effected by one of the four oxidizing species shown in Scheme 2. The Fe^{III}−OOH intermediate itself can be the oxidant (pathway **a**), or it may decompose by O−O bond heterolysis to generate a formally Fe^{V}=O species (pathway **b**) or by O−O bond homolysis to form

(43) Since the solubility of O_2 in normal organic solvent is around 0.015 M/atm partial pressure of O_2 (ref 40), the concentration of O_2 under our experimental conditions is around 0.003 M. Since the reaction of O_2 with simple alkyl radicals is diffusion controlled (rate constant of 10^{10} M^{-1} s^{-1} (ref 39), we can estimate the trapping rate constant of alkyl radicals by O_2 as 3×10^7 s^{-1}.

(44) Kurtz, D. M., Jr. *Chem. Rev.* **1990**, *90*, 585−606.
(45) Mekmouche, Y.; Ménage, S.; Toia-Duboc, C.; Fontecave, M.; Galey, J.-B.; Lebrun, C.; Pécaut, J. *Angew. Chem., Int. Ed.* **2001**, *40*, 949−952.
(46) Ho, R. Y. N.; Roelfes, G.; Feringa, B. L.; Que, L., Jr. *J. Am. Chem. Soc.* **1999**, *121*, 264−265.
(47) Kim, J. Ph.D. Thesis, University of Minnesota, Minneapolis, 1995; p 135.
(48) Girerd, J.-J.; Banse, F.; Simaan, A. J. *Struct. Bonding* **2000**, *97*, 145−177.

Table 5. ^{18}O-Incorporation from 1000 equiv of $H_2{}^{18}O$ on Alkane Hydroxylation by **1**/10 equiv of H_2O_2

alkane substrate	alcohol product	alcohol-^{18}O%
500 equiv of cyclohexane-d_{12}[a]	cyclohexanol-d_{11}	35(2)
500 equiv of cyclohexane[a]	cyclohexanol	29(2)
500 equiv of cyclooctane[a]	cyclooctanol	23(2)
1000 equiv of *trans*−1,2-dimethylcyclohexane	3,4- or 2,3-dimethylcyclohexanols	27(1)
	(1*R*,2*S* or 1*S*,2*R*)−1,2-dimethylcyclohexanol	6(1)
1000 equiv of *cis*−1,2-dimethylcyclohexane	(1*R*,2*R* or 1*S*,2*S*)−1,2-dimethylcyclohexanol	6(1)
10 equiv of adamantane	1-adamantanol	6(1)

[a] Intermolecular competition reactions with equal amounts of cyclohexane-d_{12}/cyclohexane or cyclohexane-d_{12}/cyclooctane.

Scheme 2. Possible Decomposition Pathways of the $[Fe^{III}((TPA)(OOH)]^{2+}$ Intermediate

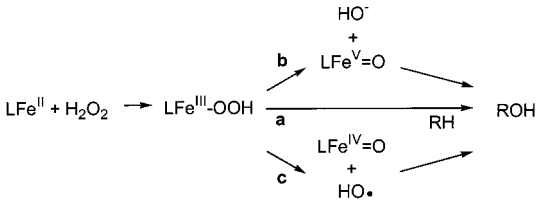

an Fe^{IV}═O species and the highly reactive HO• (pathway **c**). Since catalysts **1**−**11** all exhibit cyclohexane KIE values >3 and adamantane regioselectivities >15, the nonselective HO• can be excluded as an oxidant and pathway **c** can be eliminated as a possible mechanism. Therefore, only pathways **a** and **b** are viable for alkane hydroxylation by **1**−**11**.

Experiments carried out in the presence of $H_2{}^{18}O$ show the incorporation of ^{18}O label into the alcohol product**.** While control experiments show that the alcohols cannot exchange with solvent $H_2{}^{18}O$, the oxidation of cyclohexane by **1** and 10 equiv $H_2{}^{16}O_2$ in air in the presence of 1000 equiv $H_2{}^{18}O$ gives cyclohexanol with 27(2)% ^{18}O-incorporation. The complementary experiment with 10 equiv $H_2{}^{18}O_2$ and 1000 equiv $H_2{}^{16}O$ affords 70(5)% ^{18}O-cyclohexanol, corroborating the result for the $H_2{}^{18}O$-labeling experiment. Analogous results are also obtained for catalysts **2**−**6** (Table 4). These results exclude the direct insertion of an Fe^{III}−OOH peroxo oxygen into the alkane C−H bond as the sole mechanism for alkane hydroxylation and require the participation of a stepwise mechanism involving a species that allows an oxygen atom from solvent $H_2{}^{18}O$ to be incorporated.

One possible stepwise mechanism for water incorporation involves the intermediacy of a planar carbocation that would be susceptible to nucleophilic attack by water. This possibility can be excluded by the result of an ^{18}O-labeling experiment on the **1**-catalyzed hydroxylation of *cis*-1,2-dimethylcyclohexane; the *cis*-dimethyl stereochemistry is maintained in the tertiary alcohol product with 6(1)% incorporation of ^{18}O from water. A similar result has been reported for the stereospecific hydroxylation of *cis*-1,2-dimethylcyclohexane by **2**.[15] The retention of stereochemistry concomitant with label incorporation from $H_2{}^{18}O$ argues against a planar carbocation intermediate that would give epimerized tertiary alcohol products. Instead, these results support a mechanism involving a high-valent iron−oxo species that can exchange with solvent water, analogous to the $[(Por^{\bullet})Fe^{IV}{=}O]^{+}$ species capable of oxygen incorporation from solvent water via an "oxo-hydroxo tautomerization" mechanism.[49]

As illustrated in Scheme 3, water exchange can in principle occur at the Fe^{V}═O stage prior to C−H bond cleavage or at the Fe^{IV} stage after C−H bond cleavage. In the latter case, the exchange must be rapid enough to maintain the stereospecificity of the reaction. Furthermore, the extent of exchange should be

Scheme 3. Possible Pathways for Oxygen Exchange with the High-Valent Iron−Oxo Species

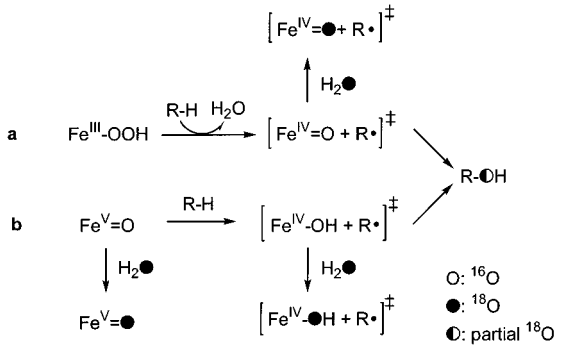

independent of the C−H bond strength since the C−H bond is already broken. In fact, our experiments summarized in Table 5 show otherwise. In intermolecular competitive oxidations of cyclohexane-d_{12} (BDE_{C-D} (bond dissociation energy) = 100.6 kcal/mol) versus cyclohexane (BDE_{C-H} = 99.3 kcal/mol) or cyclohexane-d_{12} versus cyclooctane (BDE_{C-H} = 95.7 kcal/mol),[50] less ^{18}O is incorporated into alcohols derived from the alkanes with weaker C−H bonds. Furthermore, in the intramolecular competition between the stronger secondary and the weaker tertiary C−H bonds of *trans*-1,2-dimethylcyclohexane, a greater than 4-fold difference in label incorporation is observed for the corresponding alcohols. A similarly low level of ^{18}O-incorporation is also obtained for the tertiary alcohol obtained from the oxidation of *cis*-1,2-dimethylcyclohexane or adamantane. These differences in ^{18}O-labeling may arise from steric and electronic properties of the nascent alkyl radicals that can affect the rate of C−O bond formation. However, such effects would be expected to increase the lifetime of the tertiary alkyl radical, retard the oxygen rebound rate and result in a larger ^{18}O incorporation for tertiary alcohols than secondary products, which is contrary to what is observed. Since more ^{18}O from water is incorporated into alcohols derived from the cleavage of stronger C−H bonds, there must be a competition between the incorporation of ^{18}O from water into the oxidant and the cleavage of the C−H bond. Such a competition has in fact been established in the oxidation of various alkanes by $[(Por^{\bullet})Fe^{IV}{=}O]^{+}$ in the presence of $H_2{}^{18}O$.[51] Thus, we conclude that water exchange must occur with the Fe^{V}═O species derived from **1**−**6** prior to C−H bond cleavage.

Not surprisingly, the extent of ^{18}O-labeling in the alcohol product is also dependent on the amount of $H_2{}^{18}O$ present in the reaction mixture. Figure 6 shows the results of a series of cyclohexane hydroxylation experiments conducted using catalyst **3**, chosen because it is most effective in ^{18}O incorporation from solvent water (Table 4). It is interesting to note that the fraction of $R^{18}OH$ increases linearly at lower $H_2{}^{18}O$ concentrations as

(49) Bernadou, J.; Meunier, B. *Chem. Commun.* **1998**, 2167−2173.

(50) Cook, G. K.; Mayer, J. M. *J. Am. Chem. Soc.* **1995**, *117*, 7139−7156.

(51) Goh, Y. M.; Nam, W. *Inorg. Chem.* **1999**, *38*, 914−920.

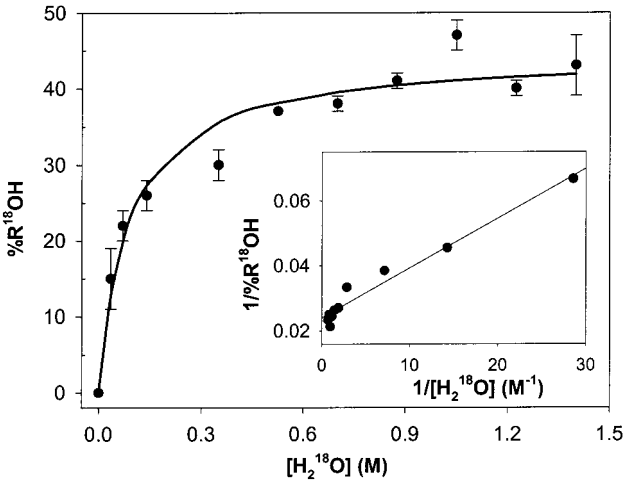

Figure 6. The fraction of ^{18}O-labeled alcohol (%R^{18}OH) obtained in cyclohexane hydroxylation catalyzed by **3**/H_2O_2 as a function of the concentration of $H_2{}^{18}O$ ([$H_2{}^{18}O$]). Inset: the double-reciprocal plot ($r^2 = 0.965$).

$H_2{}^{18}O$ concentration is increased, but reaches a plateau at higher $H_2{}^{18}O$ concentrations. A straight line is obtained when the reciprocals of both parameters are plotted, as shown in the inset, and an association constant of 16 M^{-1} can be estimated from the *x*-intercept of the double reciprocal plot. A similar saturation behavior of the %R^{18}OH value has been reported in heme-catalyzed alkane hydroxylation with 3-chloroperoxybenzoic acid (estimated association constant of 0.2 M^{-1}).[52] This saturation behavior indicates a preequilibrium binding of solvent $H_2{}^{18}O$ to the metal center prior to ^{18}O exchange with the Fe^{V}═O oxidant.

Experiments with ^{t}BuOH support the notion of preequilibrium binding of water to the metal center. In the presence of 100 equiv of ^{t}BuOH, cyclohexane hydroxylation by **1**/10 equiv of H_2O_2/1000 equiv of $H_2{}^{18}O$ affords cyclohexanol with decreased label incorporation, from 27(2)% to 19(3)%, without affecting the amount of alcohol that is formed (2.7(7) TN). This result suggests that ^{t}BuOH can compete with $H_2{}^{18}O$ for the solvent-labile site on the iron center of the metal-based oxidant and inhibit ^{18}O incorporation into the alcohol product. Indeed, we have reported mass spectral evidence for the binding of water or alcohols to related Fe^{III}−alkylperoxo species.[53]

The extent of ^{18}O incorporation from solvent water can also be modulated by substituents on the TPA ligand. As shown in Table 4, electron-donating *β*-substituents increase the amount of ^{18}O from solvent water incorporated into the alcohol product, while electron-withdrawing groups have the opposite effect. The complementary experiment with **3**/$H_2{}^{18}O_2$/$H_2{}^{16}O$ shows that, as for **1**, the balance of the oxygen in the alcohol product derives from H_2O_2 (Table 4). These observations parallel those of Goh and Nam[51] on the hydroxylation of alkanes by a series of iron porphyrins. As with the porphyrins, our results support the participation of a mechanism involving an Fe^{V}═O species. Such a high-valent species would be stabilized by an electron-rich ligand environment, and thus result in a greater ^{18}O incorporation from water.

α-Substituted Fe^{II}(TPA) catalysts on the other hand give labeling results different from those of the *β*-substituted analogues (Table 4). For complexes with two or three α-substituents (**9**−**11**), no ^{18}O from water is incorporated into the alcohol product, and the oxygen in the product derives from H_2O_2 or O_2. With only one α-substituent on the TPA ligand, **7** and **8** incorporate oxygen into the alcohol product from all three possible sources, thus representing a situation intermediate between **1**−**6** and **9**−**11**. Taken together, it is clear that the Fe^{II}-(TPA) family of catalysts affords a range of alkane hydroxylation reactivities that require invoking different metal-based oxidants to carry out C−H bond cleavage.

Scheme 4. General Mechanism Proposed for Alkane Oxidation by the Fe^{II}(TPA) Family of Catalysts in Combination with H_2O_2

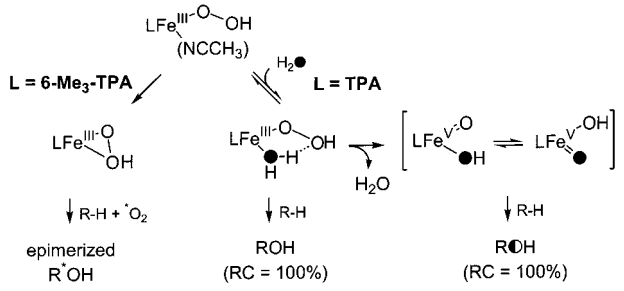

A Common Mechanistic Scheme. Scheme 4 shows a unified mechanism that derives from a consideration of all our observations. It proposes a mechanism in which both Fe^{III}−OOH and Fe^{V}═O oxidants can play a role in alkane hydroxylation (pathways **a** and **b** of Scheme 2). Summarized below are the key observations that underpin the proposed scheme:

(a) Catalysts **1**−**11** all generate oxidants that exhibit comparably high selectivity in C−H bond cleavage, that is, KIE values of 3−4 and adamantane 3°/2° ratios of 15−30.

(b) Catalysts with no α-substituents, that is, **1**−**6**, carry out stereospecific alkane hydroxylations that incorporate some oxygen derived from water into the alcohol product.

(c) The extent of solvent water incorporation depends on the strength of the alkane C−H bond: the stronger the bond, the more ^{18}O from water is incorporated.

(d) There is a fast [$H_2{}^{18}O$]-dependent preequilibrium that incorporates ^{18}O into the alcohol.

(e) Catalysts with two or three α-substituents do not incorporate ^{18}O from solvent into product and generate longer lived alkyl radicals.

In this unified scheme, the first key intermediate is an Fe^{III}−OOH species, which, depending on the particular TPA ligand, may be high-spin or low-spin. The parent TPA ligand gives rise to a low-spin intermediate, as do those with *β*-substituents, but the α-substituted TPAs favor the high-spin configuration.[21] Catalysts **7** and **8**, with only one α-substituent, are intermediate cases that afford both high-spin and low-spin peroxo intermediates, as reported for [Fe^{III}(6-Me-TPA)(OO^{t}Bu)]$^{2+}$.[21] Resonance Raman studies of such peroxo intermediates have demonstrated that the spin state of the iron(III) center has a profound effect on the strength of the O−O bond; low-spin complexes have weaker O−O bonds ($\nu_{O-O} < 800$ cm^{-1}) than high-spin complexes ($\nu_{O-O} > 850$ cm^{-1}).[21,46,48] The difference in the spin states of various Fe^{III}−OOH intermediates can be correlated with the differing alkane hydroxylation reactivities observed for the family of catalysts in this study.

Catalysts **9**−**11** with several α-substituents would be expected to form high-spin Fe^{III}−OOH intermediates.[21] The O−O bonds in such intermediates are stronger than those of low-spin counterparts, giving rise to somewhat different chemistry. The lack of ^{18}O-incorporation from $H_2{}^{18}O$ for these catalysts suggests one of two mechanistic possibilities: (a) that an Fe^{V}═O species

(52) Lim, M. H.; Lee, Y. J.; Goh, Y. M.; Nam, W.; Kim, C. *Bull. Chem. Soc. Jpn.* **1999**, *72*, 707−713.

(53) Kim, J.; Dong, Y.; Larka, E.; Que, L., Jr. *Inorg. Chem.* **1996**, *35*, 2369−2372.

(i.e., pathway **b**, Scheme 2) is not involved or (b) that pathway **b** is involved but $H_2{}^{18}O$ exchange with the Fe^{V}═O species does not occur. While we cannot exclude possibility (b), we favor possibility (a) because the steric effects of the α-substituents would very likely make attaining the Fe^{V}═O state energetically much less favorable.[21] We thus propose that alkane hydroxylation proceeds solely by the high-spin Fe^{III}−OOH active species either directly or via a stepwise mechanism involving hydrogen abstraction and radical rebound (pathway **a**, Schemes 2 and 3). However, radical rebound may be inhibited by steric hindrance of the α-substituents, allowing some of the nascent alkyl radicals to be trapped by O_2 present in solution as shown by the $^{18}O_2$-labeling results or to epimerize as indicated by the partial loss of configuration observed in the hydroxylation of the tertiary C−H bonds of *cis*-1,2-dimethylcyclohexane (Figure 4). We suggest that the η^1-OOH may be activated by the iron(III) center via isomerization to an η^2-OOH binding mode (Scheme 4), as proposed earlier to rationalize the *cis*-dihydroxylation of alkenes by **11**.[54]

Ligands with no α-substituents generate low-spin Fe^{III}−OOH intermediates, which have weakened O−O bonds[46,48] and hence a proclivity for O−O bond lysis. As proposed in Scheme 4, both the Fe^{III}−OOH and the Fe^{V}═O species derived therefrom can selectively cleave alkane C−H bonds (pathways **a** and **b**, Scheme 2). In both cases, the alkyl radical that may be formed must have a very short lifetime to account for the observed stereospecificity of *cis*-1,2-dimethylcyclohexane hydroxylation and the lack of ^{18}O-incorporation from $^{18}O_2$. While we have no evidence to exclude pathway **a**, the observation of ^{18}O-labeled alcohol products from $H_2{}^{18}O$ in the reactions catalyzed by **1**−**6** strongly argues for the involvement of the Fe^{V}═O pathway (pathway **b**).

Exchange of ^{18}O from $H_2{}^{18}O$ with the Fe^{V}═O species may occur at one of two stages. $H_2{}^{18}O$ can bind to the Fe^{V}═O species directly or enter the iron coordination sphere at the Fe^{III}−OOH stage prior to O−O bond heterolysis. Unlike the well-characterized $[(Por^{\bullet})Fe^{IV}{=}O]^{+}$ intermediate,[1,2] there is no direct spectroscopic evidence for an Fe^{V}═O intermediate in the Fe(TPA) cycle. Thus, the non-heme analogue is likely to be quite reactive and may be too short-lived to undergo sufficient oxygen atom exchange with solvent water to produce the labeling results we observe. A more attractive alternative shown in Scheme 4 involves water binding to the Fe^{III}−OOH intermediate prior to the generation of a *cis*-HO−Fe^{V}═O species. By analogy to heme systems,[49] oxo−hydroxo tautomerization of the high-valent species transfers ^{18}O from $H_2{}^{18}O$ into the terminal oxo, which is incorporated into the alcohol product.

The dual oxidant mechanism (Scheme 4) is consistent with the different extents of ^{18}O-incorporation from $H_2{}^{18}O$ observed in Tables 4 and 5. The choice of which oxidant carries out the C−H bond cleavage depends on relative rates of O−O bond cleavage versus C−H bond cleavage. The cleavage of weaker tertiary C−H bonds is mainly effected by Fe^{III}−OOH, resulting in a small amount of ^{18}O labeling from water in the tertiary alcohol products. On the other hand, the cleavage of stronger secondary C−H bonds is effected mainly by Fe^{V}═O with concomitant higher percentage of ^{18}O incorporation. Along the same lines of argument, electron-donating β-substituents on the TPA ligand favor the Fe^{V}═O channel and enhance the incorporation of ^{18}O from solvent water into the alcohol product. This dual oxidant concept has also recently gained credence in discussions of the mechanisms of methane monooxygenase,[55] cytochrome P450,[56−59] and synthetic heme catalysts.[60−64] There is thus a striking parallel in heme and non-heme iron chemistry, which earlier appeared to be quite distinct from each other but are now better construed as variations of a common mechanistic theme.

Accessing the Fe^{V}═O State without a Porphyrin Ligand. We have presented the first mechanistic evidence for a non-heme Fe^{V}═O species in stereospecific alkane hydroxylation by H_2O_2, transformations that are well established for their heme counterparts involving a $[(Por^{\bullet})Fe^{IV}{=}O]^{+}$ oxidant.[1,2,52] O−O bond heterolysis of the $(Por)Fe^{III}$−OOH species is promoted by the special properties of the porphyrin ligand, specifically its electron-rich dianionic nature and the ready accessibility of its π-cation radical state. In contrast, TPA is a neutral ligand without extensive π-conjugation. How then may the generation of the Fe^{V}═O species be enhanced in the case of $[Fe^{III}(TPA)(OOH)]^{2+}$?

We propose two features that are the key to the special reactivity of the $[Fe^{III}(TPA)(OOH)]^{2+}$ intermediate: the low-spin nature of the iron(III) center and an available coordination site *cis* to the η^1-OOH for water to bind. As suggested by both resonance Raman studies and DFT calculations,[46,48,65] the coordination of a hydroperoxide to a low-spin iron(III) center strengthens the Fe−O bond and weakens the O−O bond, thereby promoting the prospects of O−O bond lysis. O−O bond heterolysis in $(Por)Fe^{III}$−OOH species can be further enhanced by protonation of the terminal peroxo oxygen.[2,64−67] In the case of $[Fe^{III}(TPA)(OOH)(H_2O)]^{2+}$, we propose that the adjacent water ligand directs the cleavage toward O−O bond heterolysis. This water ligand can act as an acid whose acidity is enhanced by coordination to the metal center. An intramolecular hydrogen bond between the water ligand and the terminal oxygen of the adjacent HOO^{-} forms a five-membered ring (Scheme 4). Subsequent O−O bond heterolysis is facilitated by the release of a molecule of water to afford the *cis*-HO−Fe^{V}═O oxidant.

The importance of the adjacent water ligand in promoting O−O bond heterolysis is emphasized by the different reactivities of **1** and $[Fe^{II}(N4Py)(CH_3CN)]^{2+}$ (**12**).[38] N4Py is closely related to TPA, differing only by the presence of an additional pyridine ligand (Scheme 5). Like **1**, **12** reacts with H_2O_2 to form a low-spin iron(III) center with an η^1-OOH group, which also exhibits

(54) Chen, K.; Que, L., Jr. *Angew. Chem., Int. Ed.* **1999**, *38*, 2227−2229.

(55) Choi, S. Y.; Eaton, P. E.; Kopp, D. A.; Lippard, S. J.; Newcomb, M.; Shen, R. N. *J. Am. Chem. Soc.* **1999**, *121*, 12198−12199.

(56) Pratt, J. M.; Ridd, T. I.; King, L. J. *J. Chem. Soc., Chem. Commun.* **1995**, 2297−2298.

(57) (a) Vaz, A. D. N.; Pernecky, S. J.; Raner, G. M.; Coon, M. J. *Proc. Natl. Acad. Sci. U.S.A.* **1996**, *93*, 4644−4648. (b) Vaz, A. D. N.; McGinnity, D. F.; Coon, M. J. *Proc. Natl. Acad. Sci. U.S.A.* **1998**, *95*, 3555−3560.

(58) (a) Toy, P. H.; Newcomb, M.; Coon, M. J.; Vaz, A. D. N. *J. Am. Chem. Soc.* **1998**, *120*, 9718−9719. (b) Newcomb, M.; Shen, R.; Choi, S.-Y.; Toy, P. H.; Hollenberg, P. F.; Vaz, A. D. N.; Coon, M. J. *J. Am. Chem. Soc.* **2000**, *122*, 2677−2686.

(59) Collman, J. P.; Chien, A. S.; Eberspacher, T. A.; Brauman, J. I. *J. Am. Chem. Soc.* **2000**, *122*, 11098−11100.

(60) Machii, K.; Watanabe, Y.; Morishima, I. *J. Am. Chem. Soc.* **1995**, *117*, 6691−6697.

(61) Kamaraj, K.; Bandyopadhyay, D. *J. Am. Chem. Soc.* **1997**, *119*, 8099−8100.

(62) Lee, K. A.; Nam, W. *J. Am. Chem. Soc.* **1997**, *119*, 1916−1922.

(63) Lee, Y. J.; Goh, Y. M.; Han, S.-Y.; Kim, C.; Nam, W. *Chem. Lett.* **1998**, 837−838.

(64) (a) Nam, W.; Lim, M. H.; Moon, S. K.; Kim, C. *J. Am. Chem. Soc.* **2000**, *122*, 10805−10809. (b) Nam, W.; Lim, M. H.; Lee, H. J.; Kim, C. *J. Am. Chem. Soc.* **2000**, *122*, 6641−6647.

(65) Harris, D. L.; Loew, G. H. *J. Am. Chem. Soc.* **1998**, *120*, 8941−8948.

(66) Dawson, J. H. *Science* **1988**, *240*, 433−439.

(67) (a) Groves, J. T.; Watanabe, Y. *J. Am. Chem. Soc.* **1988**, *110*, 8443−8452. (b) Groves, J. T.; Watanabe, Y. *J. Am. Chem. Soc.* **1986**, *108*, 7834−7836.

Scheme 5. Structures of TPA, N4Py, and BLM[a]

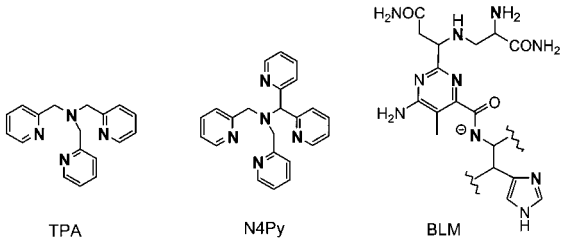

[a] The bold-face atoms represent the iron-binding ligands.

a weakened O−O bond.[46,68] But, unlike for **1**, the active oxidants in **12**-catalyzed alkane oxidation are deduced to be the Fe^{IV}═O and HO• species derived from O−O bond homolysis.[38] The distinct reactivity of the $[Fe^{III}(N4Py)(OOH)]^{2+}$ intermediate can be rationalized by the fact that N4Py is a pentadentate ligand, so there is no available site on the iron(III) center for solvent water to bind. Without the intramolecular hydrogen bond to promote heterolysis, the kinetic barrier for the formation of an Fe^{V}═O species may be too high and O−O bond homolysis occurs instead.

The antitumor drug bleomycin (BLM, Scheme 5) represents yet another variation on this theme. BLM is a pentadentate ligand like N4Py but has an amidate functionality that makes the ligand monoanionic. BLM, in conjunction with Fe^{II} and O_2, cleaves ribose 4′-C−H bonds of target DNA via a low-spin Fe^{III}−OOH intermediate called activated BLM.[69−71] Each of the three pathways in Scheme 2 has been considered to explain its reactivity.[70,72,73] Like $[Fe(N4Py)OOH]^{2+}$, activated BLM generates long-lived alkyl radicals. But unlike $[Fe(N4Py)OOH]^{2+}$, activated BLM effects regiospecific DNA C−H bond cleavage with KIE values of 2.1−4.5,[70,74] observations that exclude O−O bond homolysis (pathway **c**, Scheme 2) as the mechanism of oxidation. Furthermore, there is no compelling experimental evidence for an Fe^{V}═O species (pathway **b**),[75] a pathway also disfavored by recent spectroscopic and theoretical studies.[73] In light of the unified scheme proposed for the Fe^{II}(TPA) catalysts, we would argue that the fact that BLM, like N4Py, is a pentadentate ligand[76] prevents water binding to the low-spin iron(III) center of activated BLM and thus disfavors O−O bond heterolysis. This leaves pathway **a** as the most likely mechanism, which, like that observed for alkane hydroxylation by the $[Fe^{III}(TPA)(OOH)]^{2+}$ intermediate, exhibits a high C−H bond selectivity. Taken together, the diverse reactivities of the non-heme iron catalysts such as **1**−**11**, $[Fe^{II}(N4Py)(CH_3CN)]^{2+}$ (**12**),[38] and FeBLM[70] demonstrate how sensitive the O−O bond cleavage step is to variations in the ligand environment.

Fe^{V}═O species have been postulated in the oxygen activation mechanisms of non-heme iron enzymes such as methane monooxygenase[3] and Rieske dioxygenases.[4,9] For methane monooxygenase, intermediate **Q**, the key oxidant, is proposed to have an $Fe^{IV}_2(\mu\text{-O})_2$ core.[5] However, computational studies have suggested that this core may isomerize to an Fe^{III}−O−Fe^{V}═O unit that may actually carry out the attack of the methane C−H bond.[7,8] Rieske dioxygenases catalyze the *cis*-dihydroxylation of arene double bonds in the initial step of the biodegradation of aromatic molecules by soil bacteria but can also carry out highly stereoselective hydroxylation of aliphatic C−H bonds.[4,77−79] For example, the hydroxylation of indane by toluene or naphthalene dioxygenase affords 1-indanol with 76−100% enantiomeric excess.[78,79] Notably when this reaction is carried out in the presence of $H_2{}^{18}O$, 68% of the alcohol is ^{18}O-labeled.[78] This result provides a strong argument for the participation of an Fe^{V}═O species in the enzyme reaction. The mononuclear iron(II) center of naphthalene dioxygenase has two *cis* sites available for exogenous ligand binding,[80] which, as in the Fe^{II}(TPA) catalysts (Scheme 4), may be used to access the Fe^{V}═O state. However, the all-nitrogen ligand environment of TPA does not match the combination of histidine and carboxylate ligands found in methane monooxygenase[81] and Rieske dioxygenases,[80] so that the enzymatic mechanisms for O−O bond activation to access the Fe^{V}═O state may differ in some aspects from that proposed for the Fe^{II}(TPA) catalysts. Nevertheless, the chemistry that we have elaborated upon in this paper provides a synthetic precedent for such an Fe^{V}═O species in the oxygen activation mechanisms postulated for these non-heme iron enzymes.

Acknowledgment. This work has been supported by the National Institutes of Health (GM-33162). K.C. gratefully acknowledges a Thesis Fellowship from the Department of Chemistry of the University of Minnesota. The authors would also like to thank Professor James M. Mayer, Professor William B. Tolman, and Dr. Miquel Costas for helpful discussions, and Dr. Victor G. Young, Jr. and Dr. Maren Pink (X-ray Crystallographic Laboratory, University of Minnesota) for solving the crystal structures of complexes **3**, **4**, **8**, and **9**. We also thank a reviewer of this paper for pointing out the proper nomenclature for the tertiary alcohols of 1,2-dimethylcyclohexane.

Supporting Information Available: Table S1 of products in the oxidations of *trans*-1,2-dimethylcyclohexane and adamantane by catalysts **1**−**11** with H_2O_2; X-ray crystallographic data for **3**, **4**, **8**, and **9** (CIF). This material is available free of charge via the Internet at http://pubs.acs.org.

JA010310X

(68) Roelfes, G.; Lubben, M.; Chen, K.; Ho, R. Y. N.; Meetsma, A.; Genseberger, S.; Hermant, R. M.; Hage, R.; Mandal, S. K.; Young, V. G., Jr.; Zang, Y.; Kooijman, H.; Spek, A.; Que, L., Jr.; Feringa, B. L. *Inorg. Chem.* **1999**, *38*, 1929−1936.

(69) Burger, R. M.; Peisach, J.; Horwitz, S. B. *J. Biol. Chem.* **1981**, *256*, 11636−11644.

(70) Stubbe, J.; Kozarich, J. W. *Chem. Rev.* **1987**, *87*, 1107−1136.

(71) Sam, J. W.; Tang, X.-J.; Peisach, J. *J. Am. Chem. Soc.* **1994**, *116*, 5250−5256.

(72) Burger, R. M. *Chem. Rev.* **1998**, *98*, 1153−1169.

(73) Neese, F.; Zaleski, J. M.; Zaleski, K. L.; Solomon, E. I. *J. Am. Chem. Soc.* **2000**, *122*, 11703−11724.

(74) Kozarich, J. W.; Worth, L., Jr.; Frank, B. L.; Christner, D. F.; Vanderwall, D. E.; Stubbe, J. *Science* **1989**, *245*, 1396−1399.

(75) Heimbrook, D. C.; Carr, S. A.; Mentzer, M. A.; Long, E. C.; Hecht, S. M. *Inorg. Chem.* **1987**, *26*, 3835−3836.

(76) Wu, W.; Vanderwall, D. E.; Lui, S. M.; Tang, X.-J.; Turner, C. J.; Kozarich, J. W.; Stubbe, J. *J. Am. Chem. Soc.* **1996**, *118*, 1268−1280.

(77) Gibson, D. T.; Subramanian, V. In *Microbial Degradation of Aromatic Hydrocarbons*; Gibson, D. T., Ed.; Marcel Dekker: New York, 1984; pp 181−251.

(78) Wackett, L. P.; Kwart, L. D.; Gibson, D. T. *Biochemistry* **1988**, *27*, 1360−1367.

(79) Gibson, D. T.; Resnick, S. M.; Lee, K.; Brand, J. M.; Torok, D. S.; Wackett, L. P.; Schocken, M. J.; Haigler, B. E. *J. Bacteriol.* **1995**, *177*, 2615−2621.

(80) Kauppi, B.; Lee, K.; Carredano, E.; Parales, R. E.; Gibson, D. T.; Eklund, H.; Ramaswamy, S. *Structure* **1998**, *6*, 571−586.

(81) Rosenzweig, A. C.; Nordlund, P.; Takahara, P. M.; Frederick, C. A.; Lippard, S. J. *Chem. Biol.* **1995**, *2*, 409−418.